applied sciences

MDPI

Article

Roughness Digital Characterization and Influence on Wear of Retrieved Knee Components

Saverio Affatato [1,*], Alessandro Ruggiero [2], Silvia Logozzo [3] and Maria Cristina Valigi [3]

[1] Laboratorio di Tecnologia Medica, IRCCS Istituto Ortopedico Rizzoli, Via di Barbiano, 1/10, 40136 Bologna, Italy
[2] Department of Industrial Engineering, University of Salerno, Via Giovanni Paolo II, nr. 132, 84084 Fisciano, Italy; ruggiero@unisa.it
[3] Department of Engineering, University of Perugia, Via Goffredo Duranti, 93, 06125 Perugia, Italy; silvia.logozzo@unipg.it (S.L.); mariacristina.valigi@unipg.it (M.C.V.)
* Correspondence: affatato@tecno.ior.it

Featured Application: This paper is focused on the roughness of lateral and medial condyles used to digitally reconstruct the 3D topography of surfaces, giving insights about the wear behavior.

Abstract: Tribological performance of knee components are strongly related to the surface characteristics. Primarily, the roughness and its 3D distribution on the surfaces affect the joint performance. One of the main limitations related to the tribological study of knee prostheses is that most of the research studies report in vitro or in silico results, as knee retrievals are difficult to find or are too damaged to be analyzed. This paper is focused on the roughness characterization of retrieved metal femoral components of total knee replacements (TKR) by means of a rugosimeter and involving digital methods to reconstruct the 3D topography of the studied surfaces. The aim of this study is to investigate how changes and distribution of roughness are correlated between the medial vs. the lateral part and how the resulting digital topography can give insights about the wear behavior.

Keywords: total knee arthroplasty; digital biotribology; 3D topography; roughness characterization; wear maps

Citation: Affatato, S.; Ruggiero, A.; Logozzo, S.; Valigi, M.C. Roughness Digital Characterization and Influence on Wear of Retrieved Knee Components. *Appl. Sci.* **2021**, *11*, 11224. https://doi.org/10.3390/app112311224

Academic Editor: Alessandro Gasparetto

Received: 11 October 2021
Accepted: 23 November 2021
Published: 26 November 2021

1. Introduction

Total knee replacement (TKR) is an elective surgical procedure in orthopedic surgery worldwide to relieve pain in patients with osteoarthritis and to improve function and restore a good quality of life for patients [1]. In general, TKR consists of three main components: a metal femoral part, a metal tibial plate, and a polyethylene tibial insert. A knee replacement may fail over time and may need a second surgery for a variety of issues. Evidence from previous studies demonstrates that a TKR can last, at most, 15–20 years [2]. It is known that the success and longevity of a knee implant is affected by the characteristics of patients such as age, weight, gender, and activity level [3–6]. Surface damage and wear are the main threats to the long-term survival of a TKR [7,8]. Failure most commonly occurs due to fatigue and adhesive wear, which are responsible for the generation of micro particulate debris that, in turn, cause osteolysis around the replacements, ultimately leading to loosening and failure of the TKR [7–9]. The survival rate of total knee replacements (TKR) has been reported to increase along with the development of advanced technologies and operative techniques [10–12].

Tribological aspects of knee components are strongly related to the surface conditions. For instance, the 3D distribution of roughness and the surface topography affect the joint effectiveness. Many tribological studies regarding knee implants were performed in vitro or in silico conditions [13–16], as knee retrievals are difficult to find or are too damaged to be analyzed.

In the case of in vitro studies, the femoral or tibial inserts undergo wearing cycles at dedicated simulators in laboratory conditions, trying to replicate general motion activities, whereas in silico studies involve computational analyses of knee virtual models. In vitro and in silico tribo-characterization of prostheses are surely useful but they are rarely as predictive as in vivo studies. Nevertheless, the advantage of in vitro and in silico analyses is that all the phenomena are repeatable.

This study reports relevant damage mechanisms seen in retrieved metallic femoral components of total knee replacements accompanied with failure. Retrieved knee implants were obtained from the Register of Explant of Orthopedic Prostheses (REPO, IRCCS Istituto Ortopedico Rizzoli). To limit the effects of the prosthetic design on the roughness measurements, 18 prostheses of the same prosthetic model were selected to minimize possible confounding factors. Although most of the implants were removed due to infection, the surface analysis was essential to analyze the surface damage mode of a short-term implants. The aim of this paper is to perform a roughness characterization of the retrieved components to evaluate how changes and distribution of roughness are correlated between the medial vs. the lateral part and how the resulting digital topography can give insights about the wear behavior.

The qualitative description of the severity and location of surface damage can explain the damage mechanism on the early-retrieved implants. The surface characterization was performed using a Hommel Werke rugosimeter to evaluate the surface roughness and the texture of these components in different locations over the lateral and medial areas. The rugosimeter allowed to acquire the target surfaces point by point. In addition, a Gaussian filter was involved as a digital method to reconstruct the 3D topography of the studied surfaces, which can be read as a 3D wear map, in terms of qualitative distribution considering the strict correlation with the roughness.

2. Materials and Methods

2.1. Process of Selection

The sample implants were selected from REPO (Register of Explants of Orthopedic Prosthesis) which collects and categorizes medical devices explanted at the IRCCS Rizzoli Orthopaedic Institute (IOR). Starting from about 186 knee prosthesis explants, the largest group of prostheses with the same model was chosen by two independent observers (AM and AT) to keep a low variability and to limit the effects of the prosthetic design on the roughness measurements. Moreover, only the prostheses with particular evidence of scratches, pitting, or evident metal transfer were chosen for the analyses as the other ones were not significantly worn. In the end, 18 metallic femoral knee prostheses of the NexGen-LPS-Flex Fixed-Zimmer model, which were implanted from 2006 to 2016, remained for the roughness characterization. This kind of implant is a posterior stabilized prosthesis designed to accommodate a greater range of motion for appropriate patients. In this fixed configuration, the metallic tibial component is fixed to the tibial bone while the menisci are press-fit on the tibial plate. Major details about the sample condyles are given in Table 1.

2.2. Roughness Measurements and 3D Image Generation

The wear analysis was performed by means of surface roughness and topographic measurements. All the retrieved specimens were analyzed on three different areas, corresponding to the position of the knee during walk (30° and 60°) or at rest (0°). An area of interest of 1.5 mm × 1.5 mm (2.25 mm^2) was taken into account for each angle and on medial and lateral compartments.

Figure 1 shows the measured areas on each prosthesis.

Table 1. Specimen selection, patient characteristics, follow up, and prosthesis size-number.

Pz	Gender	Weight (kg)	Height (cm)	Side	Diagnosis	Reason for Revision	F.U. (Years)	Size
#1	F	80	160	Right	Fracture	Septic loosening	1.5	3
#2	M	94	170	Left	Unknown	Septic loosening	0.7	3
#3	M	71	170	Right	Other	Aseptic loosening	2.5	3
#4	F	74	166	Left	Aseptic loosening	Aseptic loosening	2.1	3
#5	F	78	164	Right	Arthrosis	Septic loosening	1.0	3
#6	M	106	180	Left	Arthrosis	Aseptic loosening	1.6	4
#7	M	50	NA	Left	Post-traumatic arthrosis	Septic loosening	0.2	2
#8	F	75	160	Left	Arthrosis	Septic loosening	2.5	3
#9	M	60	170	Right	Fracture	Septic loosening	1.7	3
#10	F	52	150	Left	Valgus deformity	Aseptic loosening	1.3	2
#11	M	NA	NA	Left	Arthrosis	Septic loosening	1.3	3
#12	F	74	153	Right	Other	Septic loosening	0.4	2
#13	M	95	180	Right	Arthrosis	Septic loosening	0.5	3
#14	F	107	165	Left	Arthrosis	Pain without loosening	2.1	4
#15	F	59	155	Right	Condyle necrosis	Septic loosening	0.1	3
#16	M	70	163	Right	Rigidity	Rigidity	0.6	3
#17	M	108	182	Right	Other	Aseptic loosening	4.1	4
#18	M	75	160	Right	Fracture	Septic loosening	7.6	3

Pz = patient; NA = not available; FU = follow up.

Three main roughness indices were considered to characterize the roughness of the specimens: Ra, Rt, and Rsk. The most significant indicator to characterize the surface conditions is the mean roughness, Ra, that represents the amplitude of the arithmetical mean value of the absolute values of the deviations of the real profile compared to the mean profile trace. The peak–peak height Rt is defined as the vertical distance between the highest peak and lowest valley along the measured trace for the whole analyzed surface. The Rsk represents the degree of symmetry of the surface peaks with respect to the mean plane. The values of Rsk may be:

a. Equal to zero for a normal distribution;
b. Lesser than zero for a negative distribution and a plain profile;
c. Greater than zero for a positive distribution and a profile with many peaks.

Roughness measurements were performed by means of the contact profilometer Hommel Tester T8000 (Hommel Werke, Luedinghausen, Germany), following an internal and consolidated protocol [17–20] and the following operating parameters:

- A diamond stylus tip with radius 0.020 mm;
- A measuring length of 1.5 mm;
- A cut-off of 0.25 mm;
- A travel speed of 0.15 mm/s.

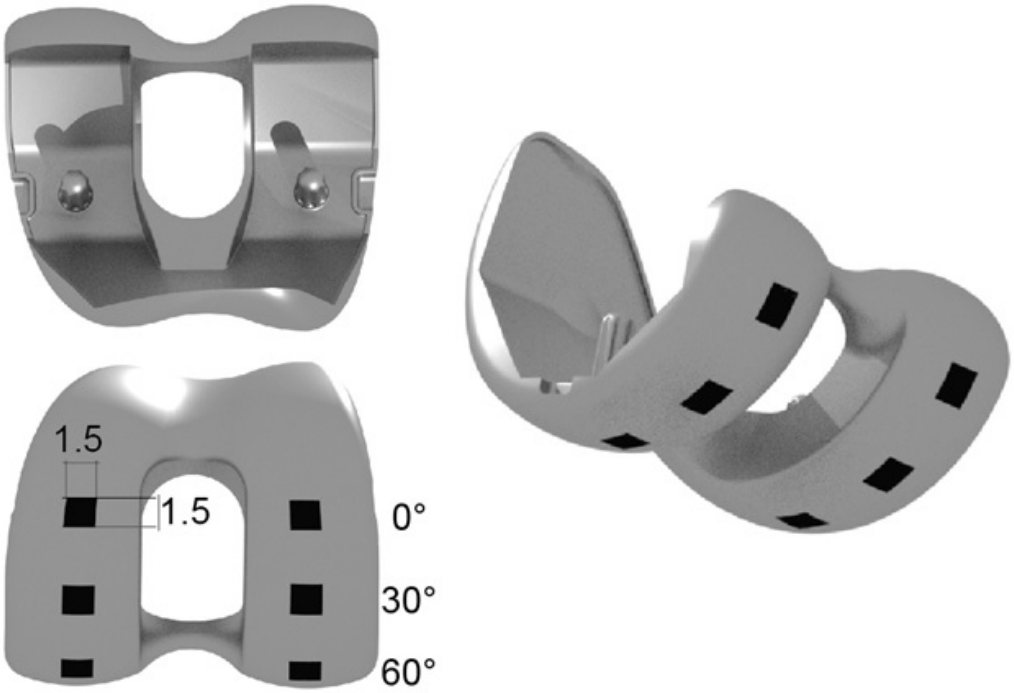

Figure 1. Areas on each femoral condyle in which were performed the roughness measurements.

All the specimens were prepared following the same procedure: before the roughness measurement, the surfaces were cleaned with acetone and then dried at room temperature in a controlled environment. Roughness was detected in A/P (antero/posterior) direction, as it was the main orientation of the scratches.

After the roughness measurements, the topographic surface acquisitions were performed on the retrievals. Three profiles were considered for each topography measured at 0°, 30°, and 60° and a 3D digital reconstruction of the worn surfaces was performed by calculating the surface topographical parameters by selecting a Gaussian filter M1 (ISO 11562) and a cut-off length of 0.250 mm, according to the recommendations in ISO 4288-1997.

The roughness filtration operator allows the mathematical separation of a surface into two new surfaces. The Gauss filtration is used for any undulation or roughness calculation that leads to a precise numerical study. This requirement complies with the recommendations of ISO 11562.

Three-dimensional topographical data give information on the wear aggression on the condyle surfaces and, in this study, they are considered as wear maps. In fact, as at the beginning of their exercise, the femoral condyles present a smooth and polished surface with roughness close to zero, the 3D distribution of Ra can be treated as a measure of the worn material, considering that the final surface level coincides with the mean profile.

2.3. Statistical Analysis

The resulting roughness values were analyzed using a non-parametric Mann–Whitney (M–W) test. Statistical significance was set at $p < 0.05$. The analyses were performed comparing the medial versus the lateral roughness measured on each condyle.

3. Results

The roughness indicators Ra, Rt, and Rsk were averaged over the repeated measurements and tabled in Table 2.

Table 2. Roughness measurements on the femoral knee retrieved components.

Pz	Ra (μm)		Rt (μm)		Rsk (μm)	
	Medial	**Lateral**	**Medial**	**Lateral**	**Medial**	**Lateral**
1	0.10 ± 0.00	0.10 ± 0.00	0.71 ± 0.37	0.45 ± 0.13	0.10 ± 0.60	0.07 ± 0.14
2	0.03 ± 0.05	0.02 ± 0.04	0.35 ± 0.08	0.35 ± 0.14	0.33 ± 0.21	0.34 ± 0.51
3	0.10 ± 0.01	0.09 ± 0.04	0.43 ± 0.22	0.45 ± 0.49	0.18 ± 0.70	0.20 ± 0.91
4	0.10 ± 0.00	0.08 ± 0.04	0.49 ± 0.14	0.46 ± 0.18	0.18 ± 0.33	−0.03 ± 0.32
5	0.12 ± 0.06	0.08 ± 0.04	0.96 ± 0.70	0.44 ± 0.11	−0.07 ± 0.86	0.34 ± 0.40
6	0.10 ± 0.00	0.10 ± 0.00	0.71 ± 0.13	0.67 ± 0.20	0.57 ± 0.39	0.58 ± 0.43
7	0.10 ± 0.01	0.08 ± 0.04	0.38 ± 0.09	0.40 ± 0.11	0.20 ± 0.13	0.27 ± 0.19
8	0.08 ± 0.04	0,08 ± 0.04	0.39 ± 0.10	0.40 ± 0.11	0.24 ± 0.20	0.17 ± 0.18
9	0.10 ± 0.00	0.12 ± 0.05	0.57 ± 0.20	1.10 ± 0.89	0.40 ± 0.48	0.35 ± 0.33
10	0.10 ± 0.00	0.10 ± 0.00	0.72 ± 0.36	0.50 ± 0.14	0.15 ± 0.90	0.19 ± 0.16
11	0.07 ± 0.05	0.06 ± 0.05	0.62 ± 0.66	0.61 ± 0.32	0.06 ± 0.93	0.23 ± 0.65
12	0.10 ± 0.01	0.10 ± 0.00	0.69 ± 0.51	0.60 ± 0.16	0.09 ± 1.12	0.06 ± 0.26
13	0.09 ± 0.03	0.09 ± 0.02	0.48 ± 0.11	0.45 ± 0.13	0.42 ± 0.34	0.41 ± 0.18
14	0.10 ± 0.00	0.10 ± 0.01	0.60 ± 0.48	0.47 ± 0.16	−0.05 ± 0.49	0.12 ± 0.23
15	0.10 ± 0.00	0.10 ± 0.00	0.53 ± 0.16	0.47 ± 0.23	0.18 ± 0.19	0.13 ± 0.30
16	0.11 ± 0.03	0.11 ± 0.05	1.10 ± 1.09	0.91 ± 1.57	0.03 ± 1.04	0.30 ± 0.82
17	0.10 ± 0.00	0.10 ± 0.02	0.56 ± 0.15	0.69 ± 0.58	−0.25 ± 0.40	0.41 ± 0.75
18	0.10 ± 0.00	0.10 ± 0.00	0.53 ± 0.28	0.65 ± 0.35	−0.14 ± 0.66	−0.20 ± 1.01

In Figures 2–4, three topographies for each condyle (medial and lateral) are shown. These pictures were obtained as an example of three patients (#pz2, #pz5, #pz16) that showed the minimum, medium, and highest Ra value. In particular, the topography picture, at a glance, represents the cumulative probability density function of the surface profile's height.

Burnishing areas and a pit distribution of approximately 1 mm in size can be found. The 3D images were reconstructed applying the Gaussian filter on the entire surface, with equal cut-off length along the two directions.

For patients #2 and #5 (Figures 2 and 3), the medial and lateral compartments showed similar wear behavior: worn surface with scratches mainly oriented along the anterior/posterior (A/P) direction on all the three areas considered for the roughness measurements. Patient #16 (Figure 4) showed less damaged surface on the lateral condyle; thin scratches along the A/P direction are visible on the medial condyle.

Regarding the statistical analyses, we found no statistical significance between the medial and lateral condyle for each roughness parameter taken into account. In particular:

Ra medial vs. Ra lateral, for each plan (0°, 30°, 60°) taken into account, showed no statistical significance ($p = 0.355$);

Rt medial vs. Rt lateral, for each plan (0°, 30°, 60°) taken into account, showed no statistical significance ($p = 0.355$);

Rsk medial vs. Rsk lateral, for each plan (0°, 30°, 60°) taken into account, showed a statistical significance ($p = 0.214$).

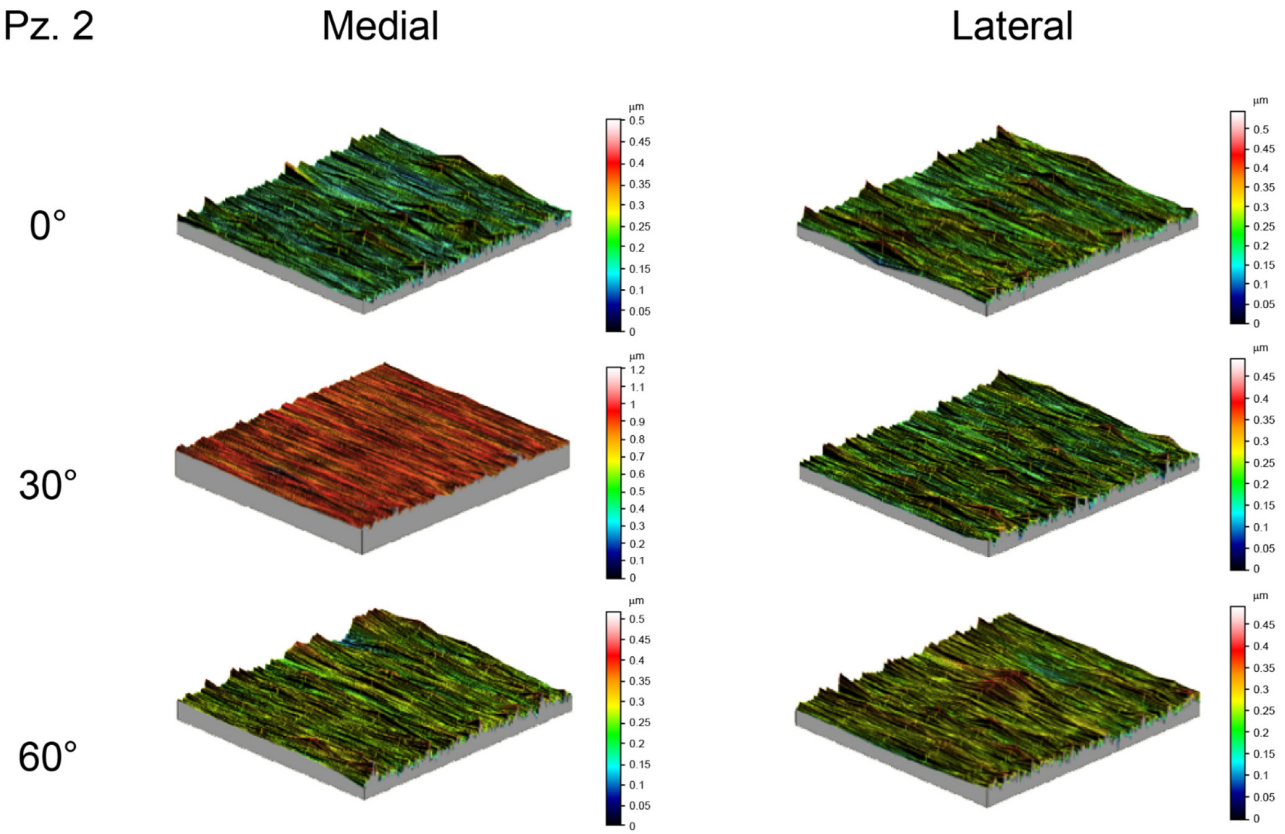

Figure 2. Topographical picture of the medial and lateral condyle with the lowest Ra value.

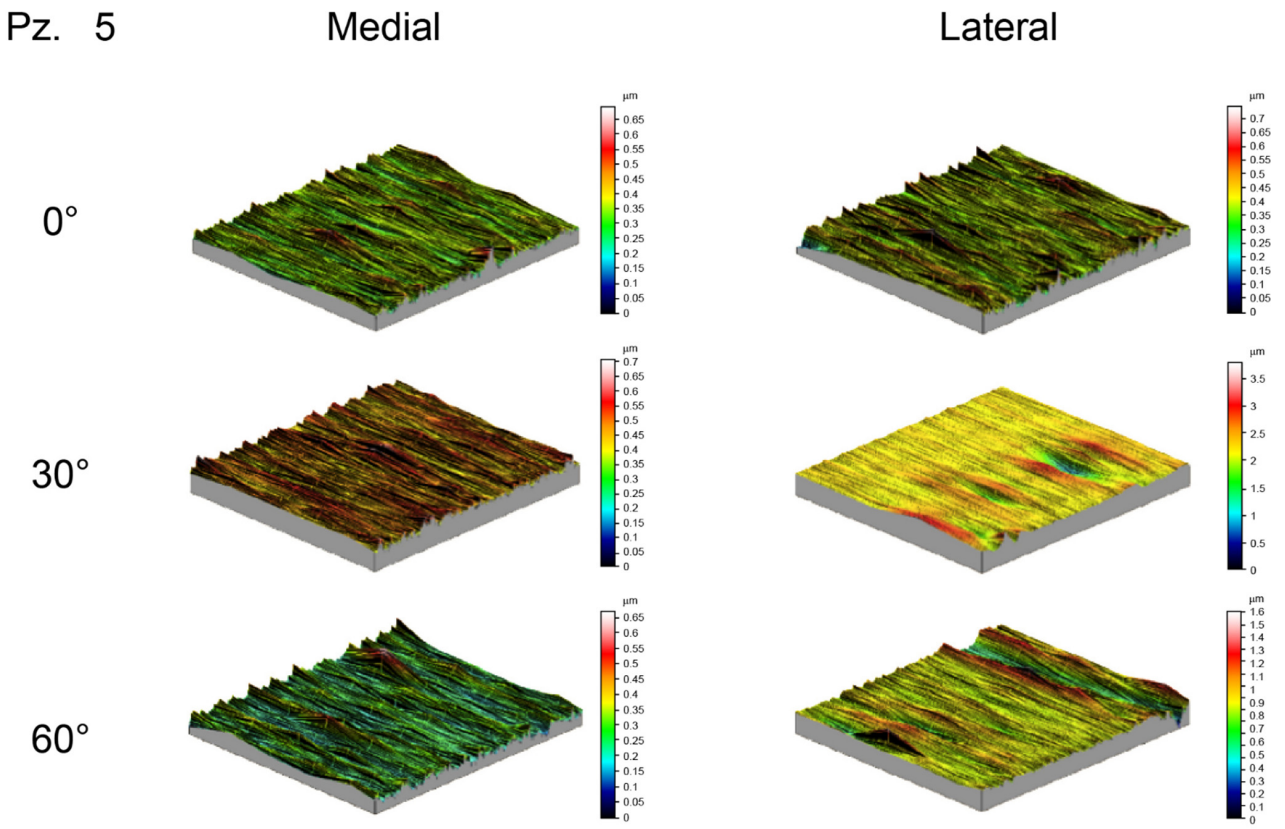

Figure 3. Topographical picture of the medial and lateral condyle with the medium Ra value.

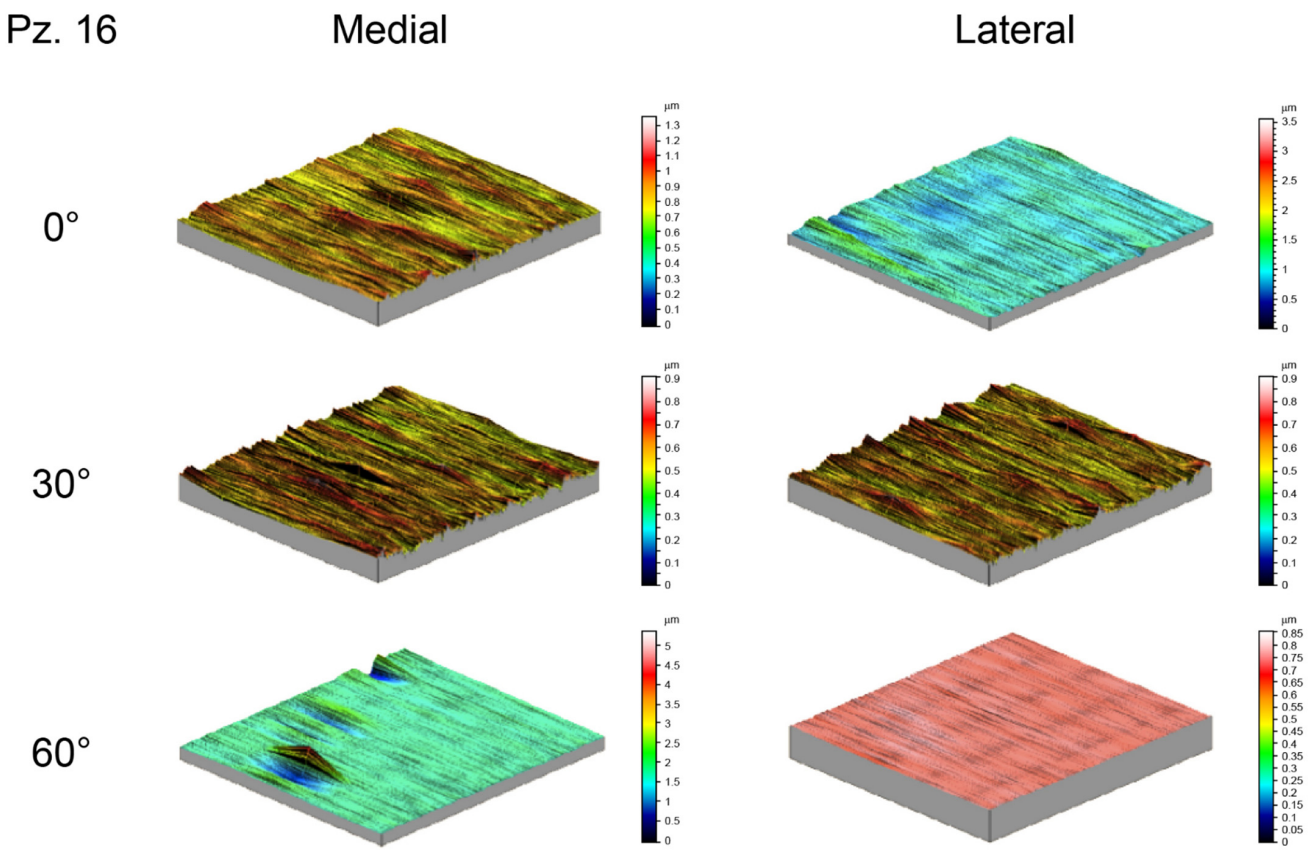

Figure 4. Topographical picture of the medial and lateral condyle with the highest Ra value.

4. Discussion

TKA is, nowadays, a well-known and widespread surgical procedure. Given the long-term problem of TKA tribological issues, surgeons are more and more interested in studies which improve in vitro tests of implants. Nevertheless, replication of in vivo wear behavior on in vitro tests remains a challenge. In this scenario, the identification of damage patterns and surface roughness distribution evaluation of retrieved components remains a crucial step to enhance the knowledge of tribological phenomena associated to the TKR exercise.

In this study, 18 retrieved TKA femoral components were selected choosing the same prosthesis design, but different sizes, to investigate surface characteristics of medial and lateral compartments. Results are given in terms of three roughness parameters (Ra, Rt, Rsk) and of 3D topographical maps of Ra, representing the worn surfaces.

Results show a non-uniform wear intensity on the two condyles. This is due to the mechanism of action of misalignments and its effect on load distribution. In fact, a varus knee alignment shifts the load-bearing axis medial to the knee center, creating a moment arm that increases forces across the medial compartment and reduces lateral load. Equally, the lateral shift of the load-bearing axis due to valgus alignment increases forces across the lateral compartment and reduces medial load. In other words, considering a standardized gait, i.e., Figure 5, it is possible to say that the increase in the valgus movement causes a varus compression and this also affects the mode of synovial lubrication of the contact surfaces [21,22].

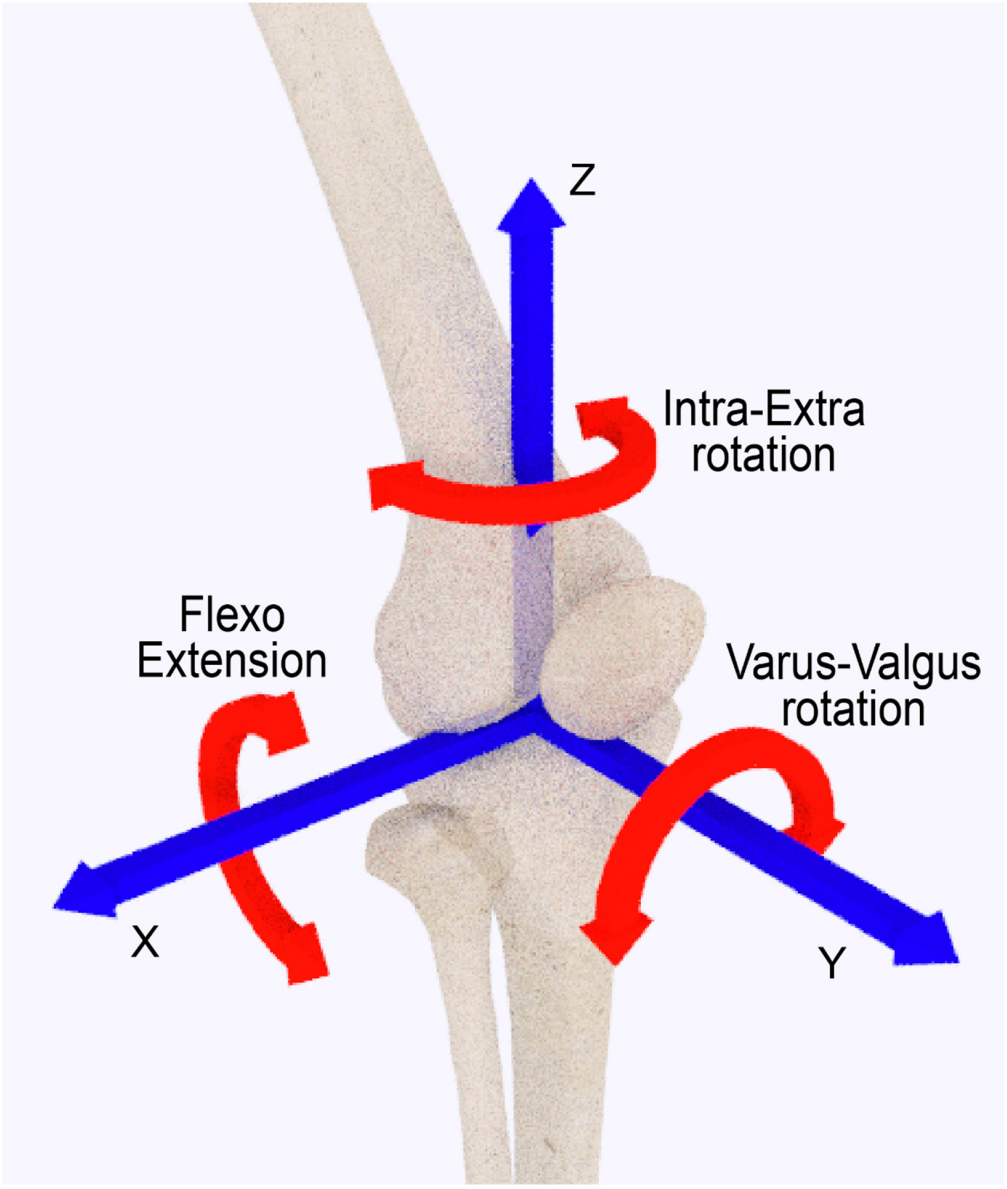

Figure 5. Tibial based TKR reference system.

It has been evidenced that surface roughness affects the wear and lubrication mechanism in total artificial joints [23,24].

In this paper, although the cause of the failure was not related to wear, the surface analysis was performed to obtain information on the surface damage mode for early implanted inserts to evaluate the early effects of in vivo exercise and provide information to understand.

This article has, obviously, some limitations. The first one is related to the low number of specimens taken into consideration in this study. The second limitation is the lack of information about measurements performed in different directions than the A/P. Further studies will be planned considering more specimens with similar characteristics (i.e., F.U., body mass index, etc.) and to measure the roughness along the medial–lateral direction at different angles.

Moreover, the measurement of contact surfaces topography plays a key role in the synovial lubrication regime acting in the artificial joints. In fact, according to Dowson et al. [25], the k parameter, calculated as the ratio between the minimum synovial meatus height and the roughness of the surfaces, could assume values lesser than 1, which is characteristic of boundary lubrication phenomena, while for $1 < k < 3$, mixed lubrication is expected.

Only in the case of k > 3, a continued film of synovial lubricant is present, which allows the complete separation of the contact surfaces with consequent low wear phenomena.

5. Conclusions

This paper presented the roughness characterization and 3D digital topographical representation of significative contact areas of retrieved knee femoral components. The study aimed at studying the wear behavior of 18 selected retrievals on the medial and lateral portions. The 3D topography of the measured surfaces was digitally reconstructed by means of a Gaussian filter, giving evidence of the wear progress over the specimen surfaces. Results show a non-uniform wear intensity on the medial and lateral condyles; however, as already demonstrated in literature, it is not possible to assess if the medial compartments surface are more worn than lateral compartments, or vice versa. Even if in this study the cause of the failure was not related to wear, this paper shows that roughness characterization of TKR early retrieved components applied as a systematic practice will help understand the wear mechanisms and causes and prevent failures due to surface damages.

Author Contributions: Conceptualization, S.A. and A.R.; methodology, S.A., A.R. and S.L.; software, S.L.; validation, S.A., A.R., S.L. and M.C.V.; investigation, S.A.; resources, S.A. and A.R.; data curation, S.L.; writing—original draft preparation, S.A.; writing—review and editing, S.A., A.R., S.L. and M.C.V.; supervision, A.R. and M.C.V.; project administration, S.A.; funding acquisition, S.A. All authors have read and agreed to the published version of the manuscript.

Funding: This research received no external funding.

Informed Consent Statement: Ethics approval was not necessary because of features of the registry, collection data as standard practice on all patients in the region, using a format protecting of the identity of the patients. Moreover, the activities of extrapolation and analysis of the RIPO (https://ripo.cineca.it (accessed on 30 September 2021)) are carried out by totally anonymizing all the data in compliance with the current legislation on privacy and confidentiality of users and operators. Data from registry are anonymized following the regional rule of Regione Emilia Romagna as regional means of public health surveillance (law 1_6_17/9).

Data Availability Statement: The data present are fully visible on the paper.

Acknowledgments: The authors thank Arianna Turchetti (Department of Biomedical Engineering, Georgia Institute of Technology, Atlanta, GA, USA) and Andrea Martelli (IRCCS Istituto Ortopedico Rizzoli) for their help with the set-up and roughness measurements.

Conflicts of Interest: The authors declare no conflict of interest.

References

1. Drexler, M.; Dwyer, T.; Chakravertty, R.; Farno, A.; Backstein, D. Assuring the happy total knee replacement patient. *Bone Jt. J.* **2013**, *95-B*, 120–123. [CrossRef]
2. Rawal, B.; Yadav, A.; Pare, V. Life Estimation of Knee Joint Prosthesis by Combined Effect of Fatigue and Wear. *Procedia Technol.* **2016**, *23*, 60–67. [CrossRef]
3. Walker-Santiago, R.; Tegethoff, J.D.; Ralston, W.M.; Keeney, J.A. Revision Total Knee Arthroplasty in Young Patients: Higher Early Reoperation and Rerevision. *J. Arthroplast.* **2020**, *36*, 653–656. [CrossRef]
4. Zanasi, S. Innovations in total knee replacement: New trends in operative treatment and changes in peri-operative management. *Eur. Orthop. Traumatol.* **2011**, *2*, 21–31. [CrossRef] [PubMed]
5. Crawford, D.A.; Adams, J.B.; Hobbs, G.R.; Berend, K.R.; Lombardi, A.V. Higher Activity Level Following Total Knee Arthroplasty Is Not Deleterious to Mid-Term Implant Survivorship. *J. Arthroplast.* **2020**, *35*, 116–120. [CrossRef] [PubMed]
6. Jenny, J.Y.; Saragaglia, D.; Bercovy, M.; Cazenave, A.; Gaillard, T.; Châtain, F.; Jolles, B.; Rouvillain, J.L. Inconsistent relationship between body weight/body mass index prior to total knee arthroplasty and the 12-year survival. *Knee* **2019**, *26*, 1372–1378. [CrossRef] [PubMed]
7. Diabb, J.; Juarez-Hernández, A.; Reyes, A.; Gonzalez-Rivera, C.; Hernandez-Rodriguez, M. Failure analysis for degradation of a polyethylene knee prosthesis component. *Eng. Fail. Anal.* **2009**, *16*, 1770–1773. [CrossRef]
8. Postler, A.; Lützner, C.; Beyer, F.; Tille, E.; Lützner, J. Analysis of Total Knee Arthroplasty revision causes. *BMC Musculoskelet. Disord.* **2018**, *19*, 55. [CrossRef]
9. Lum, Z.C.; Shieh, A.K.; Dorr, L.D. Why total knees fail-A modern perspective review. *World J. Orthop.* **2018**, *9*, 60–64. [CrossRef]

10. Rashed, S.; Lakhani, S.; Mann, A.; Best, L.M.; Shehzad, S.; Saeed, M.Z. Corrigendum to: The Impact of the Largest National Joint Registry on Current Knee Replacement Longevity Estimates: An Analysis and Review of Knee Prosthesis Brand and Fixation Technique. *J. Arthroplast.* **2021**, *36*, 3168–3173.e1. [CrossRef]
11. Mathis, D.T.; Lohrer, L.; Amsler, F.; Hirschmann, M.T. Reasons for failure in primary total knee arthroplasty—An analysis of prospectively collected registry data. *J. Orthop.* **2021**, *36*, 3168–3173. [CrossRef] [PubMed]
12. Tse, T.S.T.; Wan, Y.-C.S.; Leung, K.-H.L.; Wong, M.-K. Total knee arthroplasty: A single centre review at 10 years of follow-up. *J. Orthop. Trauma Rehabil.* **2020**, *27*, 142–147. [CrossRef]
13. Valigi, M.C.; Logozzo, S.; Affatato, S. In Vitro 3D Wear Characterization of Knee Joint Prostheses. In *Machine and Machine Science*; Springer: Cham, Germany, 2019; pp. 3855–3863. [CrossRef]
14. Affatato, S.; Bracco, P.; Costa, L.; Villa, T.; Quaglini, V.; Toni, A. In vitro wear performance of standard, crosslinked, and vitamin-E-blended UHMWPE. *J. Biomed. Mater. Res.—Part A* **2012**, *100*, 554–560. [CrossRef]
15. Affatato, S.; Ruggiero, A. A perspective on biotribology in arthroplasty: From in vitro toward the accurate In Silico wear prediction. *Appl. Sci.* **2019**, *10*, 6312. [CrossRef]
16. Affatato, S.; Valigi, M.C.; Logozzo, S. Knee Wear Assessment: 3D Scanners Used as a Consolidated Procedure. *Materials* **2020**, *13*, 2349. [CrossRef] [PubMed]
17. Affatato, S.; Grillini, L. Topography in bio-tribocorrosion. In *Bio-Tribocorrosion in Biomaterials and Medical Implants*; Woodhead Publishing: Cambridge, UK, 2013; pp. 1–21.
18. Abdel-Jaber, S.A.; Ruggiero, A.; Battaglia, S.; Affatato, S. On the Roughness Measurement on Knee Prostheses. *Int. J. Artif. Organs* **2014**, *38*, 39–44. [CrossRef]
19. Abdel-Jaber, S.; Belvedere, C.; De Mattia, J.S.; Leardini, A.; Affatato, S. A new protocol for wear testing of total knee prostheses from real joint kinematic data: Towards a scenario of realistic simulations of daily living activities. *J. Biomech.* **2016**, *49*, 2925–2931. [CrossRef]
20. Ruggiero, A.; Merola, M.; Affatato, S. On the biotribology of total knee replacement: A new roughness measurements protocol on in vivo condyles considering the dynamic loading from musculoskeletal multibody model. *Measurement* **2017**, *112*, 22–28. [CrossRef]
21. Sharma, L.; Song, J.; Dunlop, D.; Felson, D.; Lewis, C.E.; Segal, N.; Torner, J.; Cooke, T.D.V.; Hietpas, J.; Lynch, J.; et al. Varus and valgus alignment and incident and progressive knee osteoarthritis. *Ann. Rheum. Dis.* **2010**, *69*, 1940–1945. [CrossRef]
22. Tetsworth, K.; Paley, D. Malalignment and degenerative arthropathy. *Orthop. Clin. N. Am.* **1994**, *25*, 367–377. [CrossRef]
23. Welghtman, B.; Light, D. The effect of the surface finish of alumina and stainless steel on the wear rate of UHMW polyethylene. *Biomaterials* **1986**, *7*, 20–24. [CrossRef]
24. Cooper, J.R.; Dowson, D.; Fisher, J. The effect of transfer film and surface roughness on the wear of lubricated ultra-high molecular weight polyethylene. *Clin. Mater.* **1993**, *14*, 295–302. [CrossRef]
25. Jin, Z.M.; Dowson, D.; Fisher, J. Analysis of fluid film lubrication in artificial hip joint replacements with surfaces of high elastic modulus. *Proc. Inst. Mech. Eng. Part H J. Eng. Med.* **1997**, *211*, 247–256. [CrossRef] [PubMed]